ELSEVIER

Marine Geology 126 (1995) 249–269

MARINE GEOLOGY
INTERNATIONAL JOURNAL OF MARINE GEOLOGY, GEOCHEMISTRY AND GEOPHYSICS

Longshore sand waves at Southampton Beach, New York: observation and numerical simulation of their movement

Michelle M. Thevenot [a], Nicholas C. Kraus [b]

[a] *U.S. Army Engineer Waterways Experiment Station, Coastal Engineering Research Center, 3909 Halls Ferry Road, Vicksburg, MS 39180-6199, USA*

[b] *Conrad Blucher Institute for Surveying and Science, Texas A&M University–Corpus Christi, 6300 Ocean Drive, Corpus Christi, TX 78412-5503, USA*

Received 15 February 1994; revision accepted 20 December 1994

Abstract

This paper describes measurements and numerical simulations of the movement of longshore sand waves observed at Southampton Beach, Long Island, New York. These large morphologic features are created by periodic opening of a small inlet and subsequent welding of its ebb shoal to the beach. Longshore sand waves are wave-like forms that maintain identity while moving along the shore and represent a simple type of collective sediment movement or large-scale coastal behavior. Despite being described as early as 1939, few measurements of longshore sand waves have been made, and their dynamic behavior is not well understood. Eleven longshore sand waves were identified along Southampton Beach and have an average length of 0.75 km and an amplitude of 40 m. Migration speed was greatest under winter wave action and reached an average 1.09 km $year^{-1}$ and yearly average speed including summer calms was a much lower 0.35 km $year^{-1}$. During a 16-month observation period, the longshore sand waves did not disperse during their steady migration westward in the direction of predominant wave incidence, and longer waves moved faster than those with smaller wavelengths. A numerical model of shoreline change including both standard particulate longshore sand transport and a component describing migration of a longshore sand wave is developed in which the velocity of the wave is related to the calculated longshore discharge of water. The model shows wave refraction to be an important mechanism contributing to the longevity of longshore sand waves, acting to retard the otherwise expected diffusion. Model calculations of the migration of a single longshore sand wave agree quantitatively with the observations.

1. Introduction

This paper describes measurements and numerical simulations of the movement of longshore sand waves observed at Southampton Beach, on the south shore of Long Island, New York. Longshore sand waves are wave-like forms that maintain identity while moving along the shore. We associate the word "longshore" with these sand bodies to distinguish them from other morphologic wave forms that appear in navigation channels, rivers, and coastal waters, but which are not directly related to shore processes. Longshore sand waves are relatively large features and have been documented to persist over decades (Bakker, 1968) and even over a century (Verhagen, 1989), as opposed to beach cusps, which are smaller features with much shorter lifetimes on the scale of changes in wave conditions. Other terminology has been used, such as "cusp-type sand waves" (Sonu, 1968), "migrating sand humps" (Bruun, 1954; Grove et al., 1987), "accretion and erosion waves"

SSDI 0025-3227(95)00081-X

Report Documentation Page

Form Approved
OMB No. 0704-0188

1. REPORT DATE	2. REPORT TYPE	3. DATES COVERED
1995	**N/A**	**-**

4. TITLE AND SUBTITLE
Longshore Sand Waves at Southampton Beach, New York: Observationi and Numberical Simulation of their Movement

5a. CONTRACT NUMBER
5b. GRANT NUMBER
5c. PROGRAM ELEMENT NUMBER

6. AUTHOR(S)
Thevenot, Michelle M., and Krause, Ncholas C.

5d. PROJECT NUMBER
5e. TASK NUMBER
5f. WORK UNIT NUMBER

7. PERFORMING ORGANIZATION NAME(S) AND ADDRESS(ES)
U.S. Army Engineer Waterways Experiment Station, Coastal Engineering Research Center, Vicksburg, MS; Conrad Blucher Institute for Surveying and Science, Texas A&M University-Corpus Christi, Corpus Christi, TX

8. PERFORMING ORGANIZATION REPORT NUMBER

9. SPONSORING/MONITORING AGENCY NAME(S) AND ADDRESS(ES)

10. SPONSOR/MONITOR'S ACRONYM(S)
11. SPONSOR/MONITOR'S REPORT NUMBER(S)

12. DISTRIBUTION/AVAILABILITY STATEMENT
Approved for public release, distribution unlimited

13. SUPPLEMENTARY NOTES

14. ABSTRACT
This paper describes measurements and numerical simulations of the movement of eleven longshore sand waves observed at Southampton Beach, Long Island, New York. Longshore sand waves are wave-like forms that maintain identity while moving along the shore and represent a simple type of collective sediment movement or large-scale coastal behavior. These large morphologic features are created by periodic opening of a small inlet and subsequent welding of its ebb shoal to the beach. During a 16-month observation period, the longshore sand waves did not disperse during their steady migration westward in the direction of predominant wave incidence, and longer waves moved faster than those with smaller wavelengths. A numerical model of shoreline change including both standard particulate longshore sand transport and a component describing migration of a longshore sand wave is developed in which the velocity of the wave is related to the calculated longshore discharge of water. The model shows wave refraction to be an important mechanism contributing to the longevity of longshore sand waves, acting to retard the otherwise expected diffusion. Model calculations of the migration of a single longshore sand wave agree quantitatively with the observations.

15. SUBJECT TERMS

16. SECURITY CLASSIFICATION OF:			17. LIMITATION OF ABSTRACT	18. NUMBER OF PAGES	19a. NAME OF RESPONSIBLE PERSON
a. REPORT	b. ABSTRACT	c. THIS PAGE			
unclassified	**unclassified**	**unclassified**	**UU**	**21**	

(Inman, 1987), and "sand waves" (Verhagen, 1989). The terminology accretion wave and erosion wave refers to the crest of the longshore sand wave and to a situation that has been observed on the California coast of the apparent sediment blocking function of the crest, whereby a stretch of downdrift erosion precedes alongshore movement of crest (Grove et al., 1987; Inman, 1987).

Longshore sand waves have had limited study, despite being identified early in the field of coastal processes (Evans, 1939; Bruun, 1954; Sonu, 1968). More recently, the relation of longshore sand waves to beachfill response has heightened interest in the study of this simple form of large-scale coastal behavior. Longshore sand waves move on a sub-regional or regional scale and hold implications both for understanding nearshore morphology change and for engineering in the coastal zone, such as for shore-protection works and channel dredging. Bruun (1954) observed longshore sand waves along the Danish North Sea coast and distinguished them from undulatory wave features in the shoreline now referred to as beach cusps. He hypothesized that longshore sand waves moved "in the direction of the littoral drift" and that inexplicable accumulations of sediment at groin fields might be due to the arrival of a longshore sand wave. Verhagen (1989) examined a 100-year record of longshore sand waves along 20 km of Dutch coast and similarly concluded that periodic accretion in a groin field coincided with the passage of longshore sand waves and not to classical trapping of littoral (particulate) drift by the groins.

Longshore sand waves have been associated with intermittency in sand supply, as might occur through beach nourishment (Grove et al., 1987; Inman, 1987), breakup and movement of ebb-tidal shoals (Bakker, 1968), and episodic discharges of sediment from rivers (Hicks and Inman, 1987). A longshore sand wave formed by natural or artificial placement of sediment on the shoreline appears more like a solitary surface water wave than a periodic wave, often having a crest but no clear trough or wavelength. A series of longshore sand waves might at first sight look like a periodic wave, but this apparent periodicity is probably due to a cyclicity in sediment supply and not to features arising in unison and moving as a periodic wave train along the shoreline.

Longshore sand waves are a manifestation of the "collective movement" of sediment (Sonu, 1968) in which a sand body maintains morphologic identity during a life which may reach years. Collective movement should be distinguished from movement of individual sand particles. Kraus and Horikawa (1990) estimated that a typical longshore speed of a sand particle is on the order of 100 times greater than the translatory movement of longshore sand waves, which is in the approximate range of 0.3 to 4 km $year^{-1}$ (Bakker, 1968; Inman, 1987). The speed of longshore sand waves has been estimated to be inversely related to their length ℓ as $\ell^{-4/5}$ (Sonu, 1968, his fig. 11) for waves with lengths ranging from about 50 to 10,000 m. Their speed must also be related to the strength and duration of the hydrodynamic forcing, as inferred by Evans (1939), Bruun (1954), and Sonu (1968), and elaborated on below, but little information has been available to study their movement in detail.

A quantitative model of coastal morphology change must therefore be capable of describing sediment motion at two scales, relatively rapid movement of sand particles and relatively slow collective movement of large sand bodies. As a first step in developing such an approach, it is convenient to consider longshore sand waves, which to a good approximation undergo 2-D motion, and is one of the simplest manifestations of large-scale coastal behavior. Larson and Kraus (1991) showed that analytic solutions of the shoreline change equation could be modified to account for collective movement of longshore sand waves by addition of an advective term (Inman, 1987) to describe movement of the sand form. Earlier, Bakker (1968) examined a periodic solution of the shoreline equation without an advective term which was not a translatory wave but described a periodic form.

This paper describes observations and numerical simulations of longshore sand waves formed from sediment discharges issued from Mecox Inlet, an ephemeral inlet located on the southeast shore of Long Island, New York, and connecting Mecox Pond to the Atlantic Ocean. Five sets of aerial photographs show as many as 11 longshore sand

waves that were tracked over 16 months. The photographs allow estimation of the size, form, speed, and diffusion of the wave. The observations are used to examine predictions of a shoreline change numerical model developed in this study for describing the evolution of longshore sand waves.

2. Study site

The study area, Southampton Beach, is a 15-km long stretch of coastline located on the eastern end of the Atlantic Coast of Long Island, New York (Fig. 1). This stretch from Shinnecock Bay to Mecox Bay is oriented 70° east of north, and we will refer to alongshore direction as to the east or to the west. Mecox Bay is a small water body (area 6 km^2), and an inlet connecting the bay to the ocean opens periodically through storm action or through excavation. When Mecox Inlet opens, an ephemeral ebb-tidal shoal forms seaward of the inlet. This shoal migrates shoreward and in the direction of the longshore current (Zarillo and Smith, 1986), and it has been documented to weld to the shore, creating a longshore sand wave (Terchunian, 1992). Temporary openings of Mecox Inlet are manifested by as many as 11 probable longshore sand waves that appear in recent photographs. The longshore sand waves tend to move westward, in the predominant direction of littoral drift, until they merge with the updrift impoundment fillet at the east jetty of Shinnecock Inlet. Mecox Inlet is the westernmost in a series of three ephemeral inlets along the

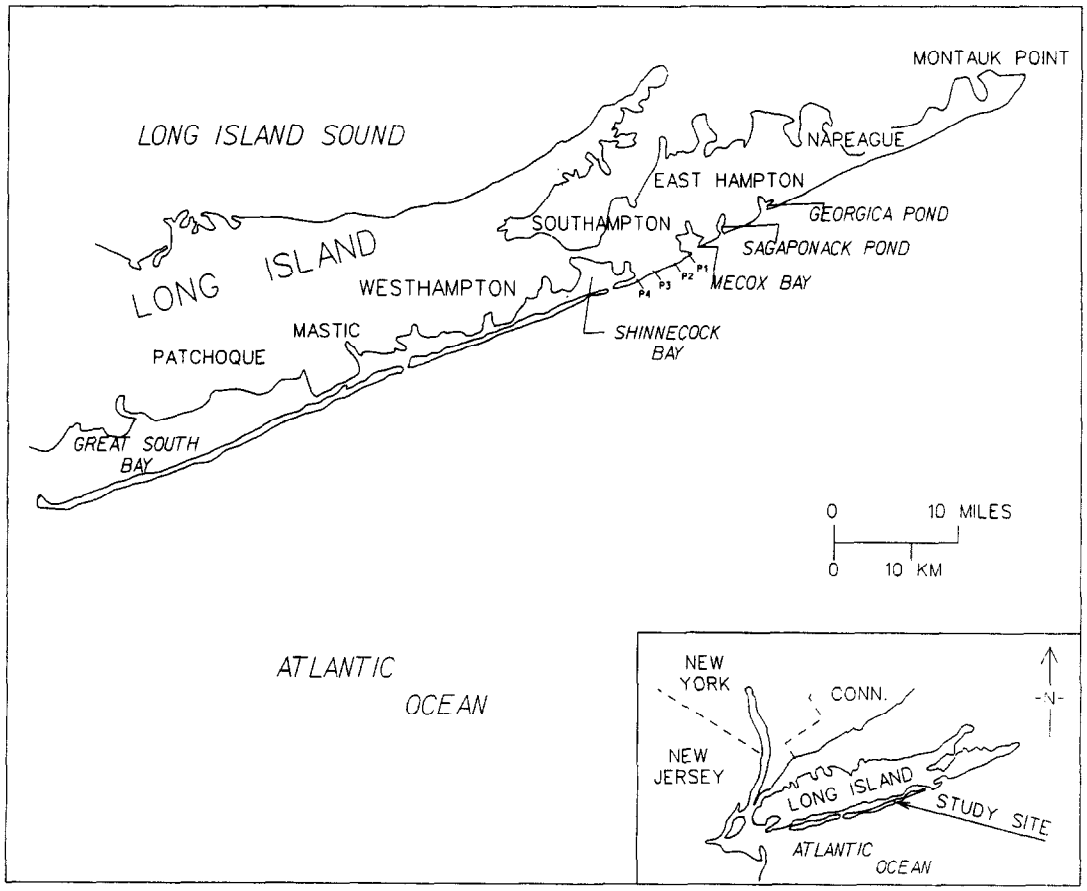

Fig. 1. Location map for Southampton Beach.

eastern end of Long Island which create longshore sand waves that migrate along the shore. Longshore sand waves observed updrift of Mecox Inlet are created by Sagaponack Pond, located 4 km east of Mecox Bay, intermittently opening to the Atlantic Ocean. Georgica Pond, located 7 km east of Sagaponack Pond, also releases migrating sand waves.

The beaches along the south shore of Long Island are composed mainly of quartz sand with some garnetiferous and magnetic sands and shell fragments (Leatherman and Allen, 1985). The sand tends to be fine-to-medium grained with a median grain size of 0.25 mm (Nersesian et al., 1992). The beach width at Southampton ranges from 50 to 200 m with a dune elevation of approximately 5 to 8 m National Geodetic Vertical Datum (NGVD). Typical beach profiles (Lockwood, Kessler and Bartlett, 1979) shown in Fig. 2 (locations shown in Fig. 1), illustrate a beach face slope of approximately 1 m vertical to 10 m horizontal. Two bars are observed; a nearshore bar located approximately 100 m offshore, and a bar 300 to 400 m offshore. Shoreline position was adjusted to a common datum (NGVD) by applying a correction for tide level at the time of photography as estimated by the National Ocean Survey (1992) tide data and by translating the shorelines based on an average foreshore slope taken from the beach profile data (Fig. 2). The tide is semi-diurnal with mean range of 0.9 m and spring range of 1.1 m.

Average waves at the study site have significant height of approximately 1.0 m and a period of about 8 sec, according to a recent 20-year Wave Information Study (WIS) hindcast (Hubertz et al., 1993). The predominant wave direction is toward the west. Seasonal fluctuations include larger westerly waves typically occurring from autumn through spring, and smaller waves, directed toward the east, typically occurring in summer. The resulting net potential longshore transport rate along Long Island has been estimated from impounded volumes at jetties to be 300,000 m^3 $year^{-1}$ to the west (Panuzio, 1968). Time series wave data used in the present study were taken from Sep. 1956 to Jan. 1958 of the WIS hindcast, with values of wave height, period, and direction available at 3-h intervals. These data were selected because they were representative of the seasonal variability of wave conditions shown in the 20 years of WIS data.

3. Observed longshore sand waves

3.1. Identification of longshore sand waves

Five recent sets of vertical aerial photographs (four sets in color, one in black and white) were obtained showing longshore sand waves along

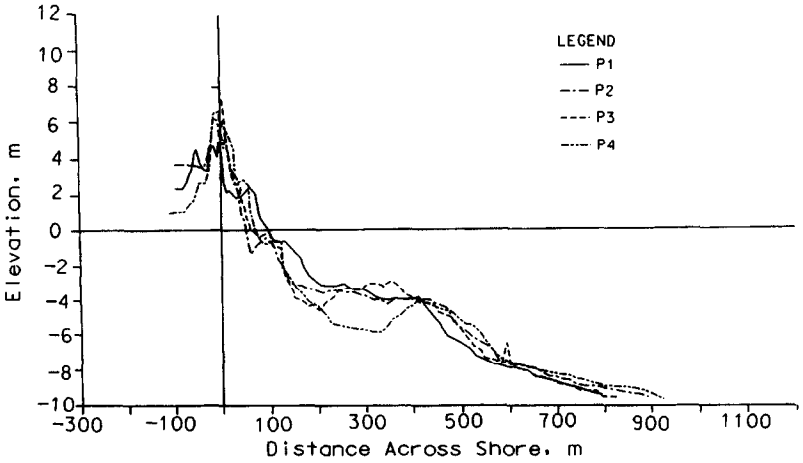

Fig. 2. Representative beach profile shape at Southampton.

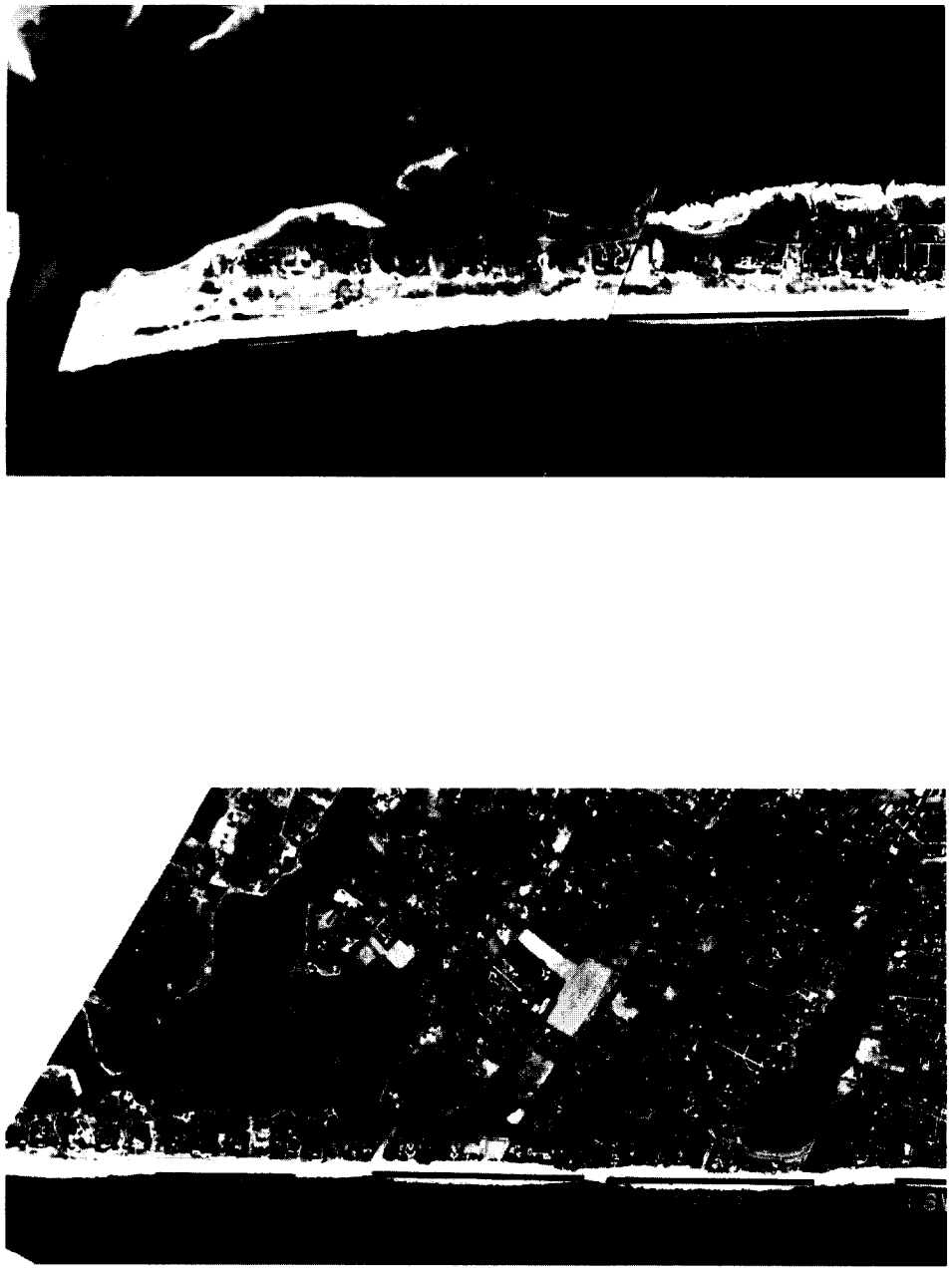

Fig. 3. Study reach, Mar. 29, 1992, showing 11 longshore sand waves.

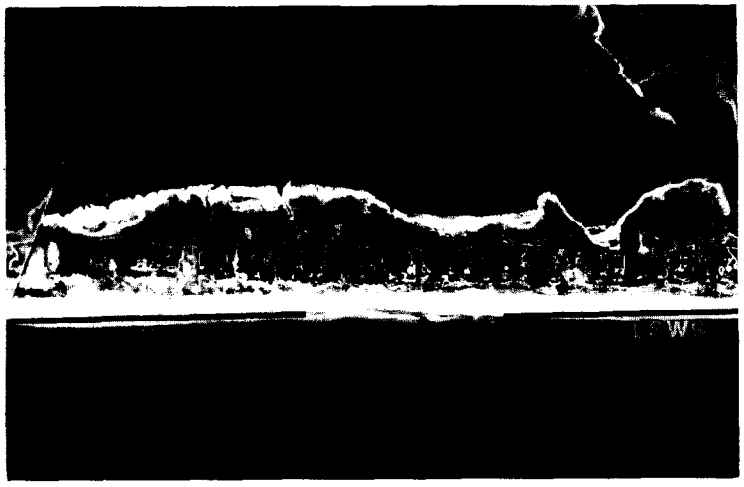

aves.

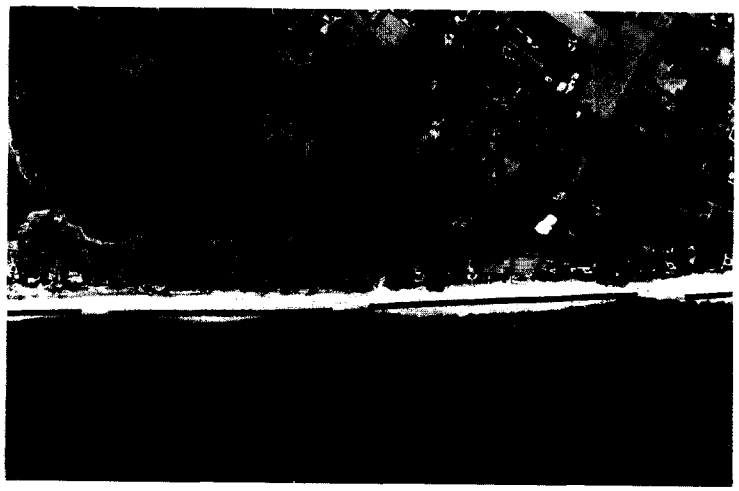

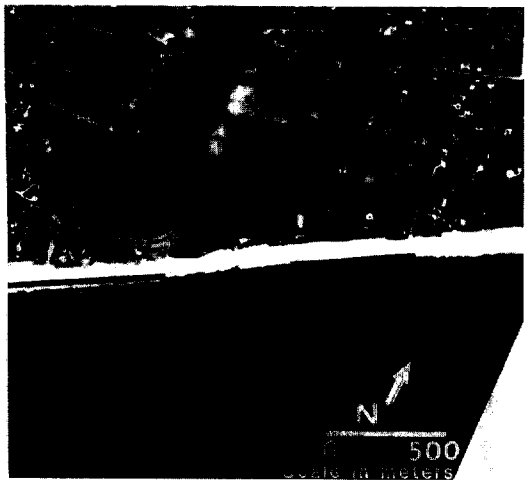
N
500
Scale in meters

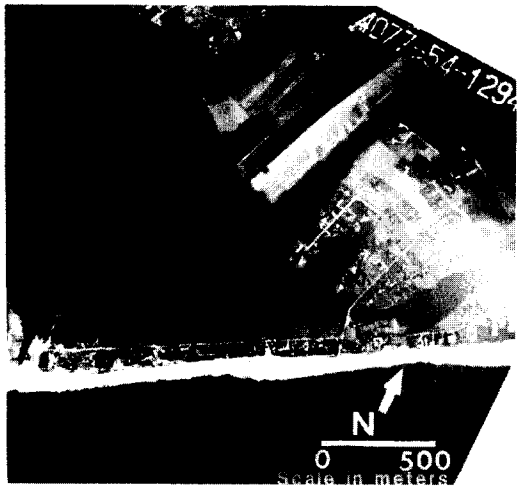
A077-54-129
N
0
500
Scale in meters

Southampton Beach over the 16-month interval from Sep. 1991 to Jan. 1993. Photographs dated Sep. 4, 1991, Dec. 20, 1991, Dec. 18, 1992, and Jan. 2, 1993 are at a scale of 1:12,000 and were taken by TopoMetrics, Inc. An additional set of photographs taken by Lockwood, Kessler, and Bartlett, Inc., dated Mar. 29, 1992 is at a scale of 1:19,200.

Fig. 3 shows the locations of the 11 longshore sand waves identified for analysis, giving approximately one wave per 1.5 km of shoreline. To be considered for quantitative analysis in this study, a longshore sand wave (abbreviated as LSW when numbered) had to be clearly discernable in at least three of the five sets of photographs. LSW 3 was directly identified by Terchunian (1992) as created by a particular opening and closing of Mecox Inlet. It is noted from Fig. 3 that longshore sand waves tend to be asymmetric, with a steeper flank downdrift of the predominant direction of current (which is to the west), similar in shape to a subaqueous sand wave or dune subjected to unidirectional flow. Other researchers have made use of the analogy between longshore sand waves and dunes, including Evans (1939), Bruun (1954), and Sonu (1968). In the present case, with the longshore current acting as an analogue for unidirectional flow, the steeper flank lies to the west.

Fig. 4 shows the shoreline and interpreted subaqueous morphology of longshore sand waves inferred from the aerial photographs. Predominant features include the dune line, land–water interface, and nearshore morphology. The dune line is stationary except when impacted by severe storms. The summer beach is about 50 m wider than the winter beach. The subaqueous morphology associated with sand waves appears as oblique finger shoals which may protrude as far as 500 m offshore and are oriented downdrift from the beach. Similar finger shoals described by Sonu (1968) were also skewed in the direction of the longshore current. The shoals in Fig. 4 are distinguished as discolor-

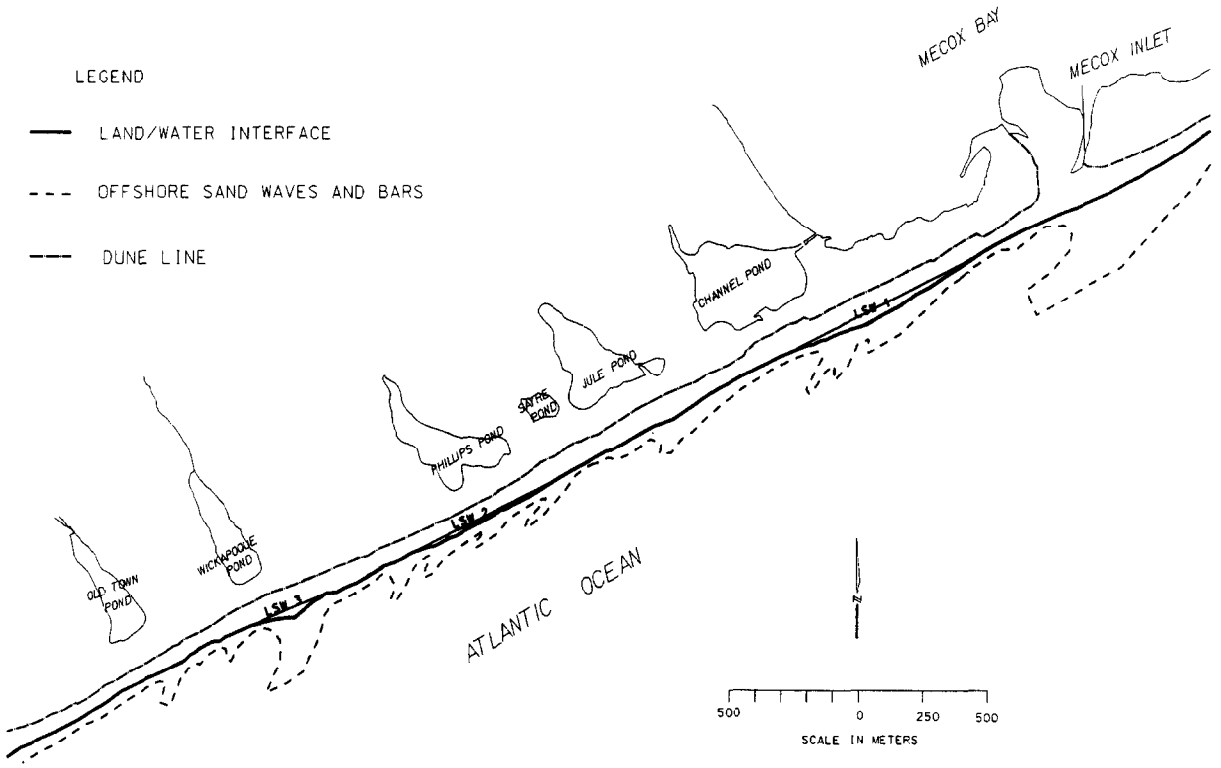

Fig. 4. Plan view interpretation of nearshore morphology.

ations in the water adjacent to many of the longshore sand waves at Southampton. The associated bathymetry creates a protected environment for the longshore sand waves as seen by converging breaking waves at their crests (Fig. 5), and convergence of the breaking waves is considered as being a major contributor to the preservation of the longshore sand waves.

Three sets of aerial photographs were selected for morphologic analysis and quantification of the motion of the 11 longshore sand waves. The Sep. 4, 1991 set of photographs served as an initial reference condition. Photographs taken on Dec. 20, 1991 were chosen to isolate the winter period (from Sep. to Dec.) for determining seasonal differences in longshore sand wave migration speed. The Jan. 2, 1993 set of photographs was selected because it was the final available data set, and it showed less shoreline damage caused by a major storm in Dec. 1992 than the photographs taken that same month.

3.2. Characterization of LSW geometry

The observed longshore sand waves were characterized as solitary waves. As shown in Fig. 5, a wave amplitude η (maximum distance from baseline of mean local shoreline position) and a wavelength λ (distance over which the wave protrudes from the mean shoreline position) were scaled from each of the three selected sets of photographs. An absolute measurement accuracy of ± 3.5 m can be expected from the technique used. A threshold value of amplitude of 20 m was applied in identifying longshore sand waves, representing an estimated accuracy in feature identification. A certain degree of interpretation is required in determining the amplitude of the longshore sand waves, as some were occasionally bimodal, having two points which could be identified as crest. Ambiguity in determining amplitude adds inaccuracy in some of the measurements.

A mean velocity V for each longshore sand wave was determined for the Dec. 20, 1991 and Jan. 2, 1993 data as the direction and distance that the crest of the wave had moved over the time elapsed since Sep. 4, 1991. For example, LSW 3 moved from a position clearly east of the nearby housing subdivision on Sep. 4, 1991 (see reference line on Fig. 5) to a location adjacent to the subdivision on Dec. 20, 1991 (Fig. 6), a displacement of more than 200 m in approximately 3.5 months. Fig. 7 shows LSW 3 on Jan. 2, 1993 to lie west of the subdivision, a total migration distance of nearly 300 m. LSW 3 is typical in that the mean migration speed was three times greater in the winter

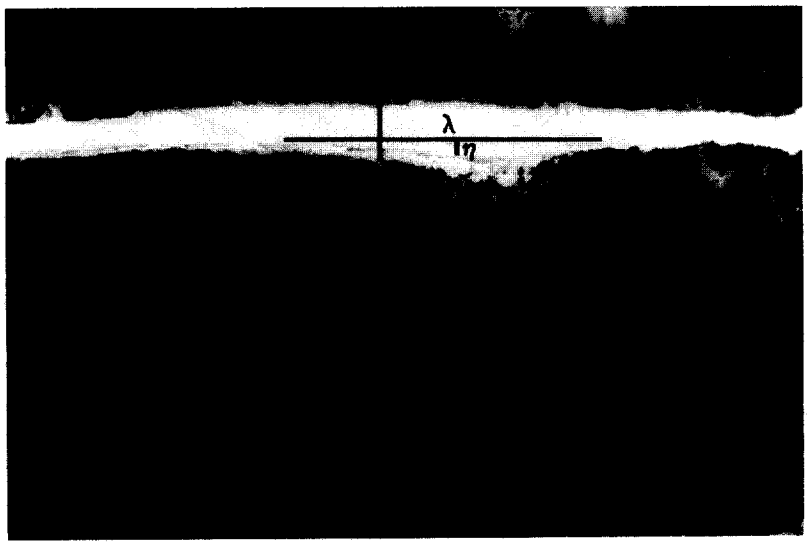

Fig. 5. Longshore Sand Wave 3, Sep. 4, 1991.

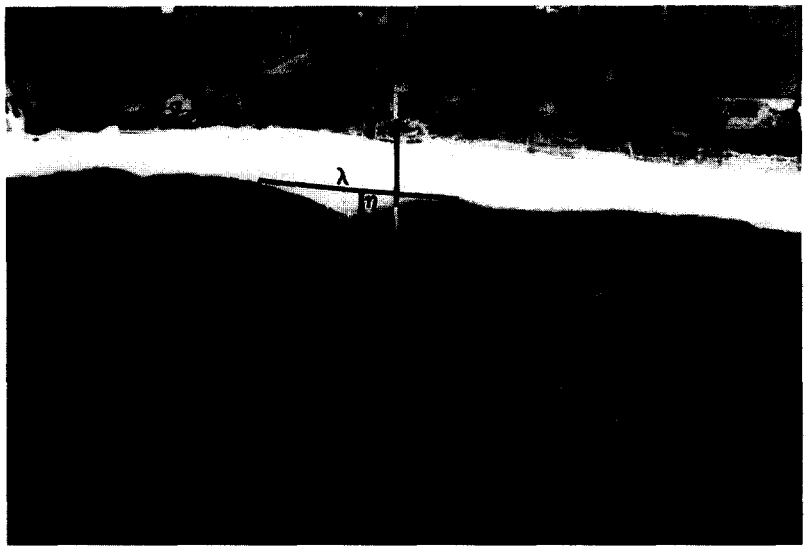

Fig. 6. Longshore Sand Wave 3, Dec. 20, 1991.

Fig. 7. Longshore Sand Wave 3, Jan. 2, 1993.

(Sep. 4, 1991 to Dec. 20, 1991) than during the 16-month period (Sep. 4, 1991 to Jan. 2, 1993) that included summer. Table 1 lists values of η, λ, and V for the three sets of photographs, including mean values for each time interval.

LSW 10 does not appear in the photographs of Jan. 2, 1993, and it is thought that LSW 10 was overtaken and engulfed by the faster moving LSW 9. The photographs indicated that if a wave moved at a speed 0.70 km year^{-1} slower than the next consecutive easterly (updrift) wave in the Dec. 20, 1991, it would combine with the faster moving updrift wave to form one wave by Jan. 2, 1993, similar to the fate of LSW 10. LSWs 5 and 8 were shown in the Dec. 20, 1991 data to migrate at speeds 0.75 and 0.72 km year^{-1} slower than LSWs 4 and 7, respectively. Thus, neither LSW 5 nor LSW 8 was observed in the Jan. 2, 1993 photo-

Table 1
Amplitude η, length λ, and velocity V of longshore sand waves observed at Southampton Beach, Long Island, New York. (Positive velocity means movement toward west.)

Sep. 4, 1991			Dec. 20, 1991			Jan. 2, 1993		
LSW	η (m)	λ (m)	V (km yr^{-1})	η (m)	λ (m)	V (km yr^{-1})	η (m)	λ (m)
1	56	577	0.37	62	812	0.29	62	880
2	42	717	1.32	28	802	0.36	90	1133
3	42	750	0.85	48	425	0.2	28	558
4	35	840	1.32	35	277	0.24	77	1165
5	28	513	0.57	35	398	–	–	–
6	56	1030	1.18	49	1377	0.43	62	1175
7	33	527	1.76	49	1358	0.42	62	1422
8	42	994	1.04	28	1308	–	–	–
9	42	758	2.18	39	530	0.52	69	1528
10	35	1217	0.49	56	940	–	–	–
11	21	285	0.97	28	342	–	–	–
Ave.	39	746	1.09	41	779	0.35	64	1130

graphs. LSW 11 also does not appear in the photographs of Jan. 2, 1993; the speed of LSW 11 was below the threshold and would be expected to combine with LSW 9 which was moving more than 1 km year^{-1} faster. LSW 11 was approaching the east jetty at Shinnecock Inlet, and the wave speed was probably reduced through the orientation of the fillet adjacent to the jetty, which would produce a weaker longshore current because of smaller angles of wave breaking to the local shoreline.

A relatively strong linear relationship (correlation coefficient of 0.84; significant to 95% confidence interval) between observed λ and V was found for the Sep. 1991–Jan. 1993 data. These data indicate that the longer longshore sand waves move faster than the shorter ones, in contrast to the observations of Sonu (1968), who postulated that the longshore velocity of sand bodies would vary inversely with the wavelength as $\lambda^{-4/5}$. If three of the seven points denoting combined waves are removed, the correlation is 0.97 for the remaining four points. No such trend was found for the Sep. 1991–Dec. 1991, probably because of the short time period of observation.

Of the 11 longshore sand waves observed at Southampton, three increased in both amplitude and length between the period from Sep. 4, 1991 and Dec. 20, 1991. Three sand waves increased in amplitude while decreasing in length, and three sand waves increased in wavelength while decreasing in amplitude during this period. One sand wave decreased in both amplitude and length, and another sand wave maintained the same amplitude and decreased in wavelength. These data suggest that no obvious trend exists between magnitude of amplitude and wavelength over the 3.5-month period. However, between Sep. 4, 1991 and Jan. 2, 1993, six of the seven visible sand waves increased in both amplitude and wavelength. Of these six sand waves, three would be expected to increase in volume because they had engulfed one or more other waves. The remaining sand wave, LSW 3, was observed on Jan. 2, 1993, to decrease in both amplitude and wavelength. Overall, the 16-month observation period indicates a tendency for longshore sand waves at Southampton to maintain form and increase in subaerial volume.

Inman (1987) observed that a longshore sand wave along the coast of California tended to diffuse by decreasing in amplitude while increasing in length. However, the longshore sand waves migrating along the Long Island coast tended to slightly increase in amplitude and length. The sand wave observed by Inman (1987) was produced by the artificial injection of 600,000 m^3 of sandy material to the littoral system. Strong dispersion would be expected of this non-equilibrated system. In con-

trast, the longshore sand waves produced at Mecox Inlet are, by the naturally occurring processes, scaled to the width of the surf zone and to the energy of the incident waves, suggesting that they may be close to an equilibrium form that can preserve identity.

4. Numerical simulation

4.1. Mathematical approach and analytical formulations

In this section we provide background for the numerical approach that follows by considering some general properties of analytical solutions to the equation governing shoreline change. Mathematical modeling of coastal shoreline change was originated by Pelnard-Considere (1956), and such modeling has become a standard engineering technique for predicting the long-term (order of years to decades) evolution of the position and shape of the shoreline. Three basic assumptions underlie shoreline change models (Hanson and Kraus, 1989): (1) long-term permanency of the beach profile shape (implying the existence of an equilibrium form); (2) existence of a depth of closure of sediment movement; and (3) dependence of the sand transport rate on wave direction (which determines the direction of the mean longshore current moving the sand).

If the assumptions are made that the incident waves are constant in height and direction alongshore and through time, and that they arrive at a small angle to the trend of the coast, closed-form analytic solutions are available (e.g., Pelnard-Considere, 1956; Larson et al., 1987). For this simple case, the equation governing change in the shoreline position y, derived from conservation of sand, reduces to the 1-D diffusion equation:

$$\frac{\partial y}{\partial t}=\varepsilon\frac{\partial^2 y}{\partial x^2} \tag{1}$$

in which the shoreline position y is a function of the distance x along the shore and the time t, and ε is an empirical coefficient related to the particular predictive longshore sand transport rate formula and the depth of closure (depth to which the beach profile moves when the shoreline moves). Numerous useful closed-form or analytical solutions can be found for Eq. 1 (Larson et al., 1987); however, this equation describes diffusion which tends to obliterate the distinct and persistent shoreline sand forms which are addressed in this study.

In recent years, interest has heightened in what Sonu (1968) called collective movement of sand, in which large bodies having the dimensions on the order of the width of the surf zone move alongshore. The longshore movement of large sand forms can be incorporated in Eq. 1 by including a form advective term $V(\partial y/\partial x)$ (Inman, 1987; Larson and Kraus, 1991), which can be derived as in forming the standard advection–diffusion equation for a conservative substance, to give:

$$\frac{\partial y}{\partial t}+V\frac{\partial y}{\partial x}=\varepsilon\frac{\partial^2 y}{\partial x^2} \tag{2}$$

in which V is the migration speed of the sand wave and is presumably a function of the hydrodynamic conditions, which vary in time and also depend on the offshore bathymetry.

No predictive expressions are available to specify V, although Sonu (1968) deduced that the migration speed of "sinuous shorelines and crescentic bars" was a function of spacing of the forms, with larger bodies moving more slowly. Sand wave speed on the southern coast of California have been reported in the range of 0.5 to 4 km year^{-1} (Grove et al., 1987; Inman, 1987). Similar values have been found by others for large sand protrusions moving alongshore and establish the order of magnitude for V. The speed V is taken as a constant for obtaining simple analytic solutions for Eq. 2. As shown by Larson and Kraus (1991), if the transformation is made to a coordinate system moving in the positive x direction with speed V by defining arguments $\phi=Vt-x$ and $\theta=t$, then by the chain rule of differentiation, Eq. 2 reduces to the same form as Eq. 1 (let ϕ go to x and θ go to t). Therefore, if there are no disturbances at the boundaries, analytical solutions of Eq. 1 are also solutions of Eq. 2, but with the arguments ϕ and θ. Eq. 2 thus describes the migration of a sand body with a characteristic velocity

V that tends to diffuse and lose identity. A numerical solution is required to achieve more generality such as feedback of bathymetry to the forcing waves and to allow time-varying and longshore-varying wave conditions, described in the next section.

In Eq. 2, the term proportional to V represents the movement of a shoreline form, such as longshore sand waves, and the term on the right side represents shoreline change produced by particulate motion. Let us set $\varepsilon = 0$, implying no individual particulate motion, giving:

$$\frac{\partial y}{\partial t} + V\frac{\partial y}{\partial x} = 0 \tag{3}$$

A periodic or wave-like solution (longshore sand wave) to this equation is:

$$y = \eta_{\max} \cos\left(\frac{2\pi}{\lambda}x - \frac{2\pi}{\tau}t\right) \tag{4}$$

in which $\eta_{\max}$ is the amplitude of the sand wave, λ is the wavelength of the sand body, and τ is the period of the wave.

Closed-form solutions require further simplifications, the major ones being a schematic initial shape of the shoreline feature and waves of constant height and direction through time and alongshore. Therefore, to allow generality and to more realistically represent time-varying waves, wave transformation across shore, and migration and evolution of a longshore sand wave, a numerical shoreline change simulation model was developed.

4.2. Shoreline change and sand transport

If the particulate transport rate Q_P is given by the "CERC" formula (Shore Protection Manual, 1984), then $Q_P = Q_0 \sin(2\theta_b)$ in which θ_b is the angle of the breaking wave crests to the trend of the local shoreline, and Q_0 the amplitude of the longshore sand transport rate (Larson et al., 1987). With this choice of the longshore sand transport rate formula, ε becomes $\varepsilon = 2Q_0/D_c$ in which D_c is the depth of closure, and $\partial^2 y/\partial x^2 = (2Q_0)^{-1}\partial Q_P/\partial x$. The preceding substitutions into Eq. 2 result in the equation governing the movement of longshore sand waves used in the numerical model:

$$\frac{\partial y}{\partial t} + V\frac{\partial y}{\partial x} = \frac{1}{D_c}\frac{\partial Q_P}{\partial x} \tag{5}$$

The second term on the left side of Eq. 5 is an advection term that governs the movement of the longshore sand wave.

The dependence of V on possible governing variables has not been previously examined, and an estimation method to calculate it in the model had to be developed in the present study. One expects with Bruun (1954) and others that a longshore sand wave should move in the direction of the littoral drift or with the longshore current. One would also expect that a stronger current would cause more rapid movement. What is "strong?"

In measurements of sand waves in uniform flow of the upper part of an estuary, Nasner (1974, his fig. 5) found a well-defined linear relation between the speed of sand waves (or dunes) in the Weser River, Germany, and the mean freshwater discharge that occurred between depth soundings. Kraus and Dean (1987) found correlation between the measured particulate longshore sand transport rate and the longshore discharge of water in the surf zone at Duck, North Carolina, facing the Atlantic Ocean. Here, we associate the speed of a longshore sand wave with the longshore discharge of water rather than with longshore current speed (such as the mean current speed).

Following Kraus and Dean (1987), a longshore water discharge parameter R is defined as:

$$R = \frac{1}{2} d_b y_b v_{ls} \tag{6}$$

in which d_b is the depth at wave breaking, y_b is the distance from the shoreline to the break point, and v_{ls} is the mean velocity of the longshore current. The wave transformation model takes waves over locally straight and parallel contours from offshore to the break point, and the assumption of a beach profile shape allows calculation of d_b and y_b. The longshore current velocity can also be calculated from parameters given by the wave

model as:

$$v_{ls} = \frac{1.35}{2} \gamma \sqrt{g d_b} \sin(2\theta_b) \quad (7)$$

Eq. 7 is an empirical expression found by Komar and Inman (1970) in their longshore sand transport tracer field experiments, in which γ is ratio of wave height to water depth at breaking, g is acceleration due to gravity, and θ_b is angle of wave crests at breaking to the local shoreline.

The volume rate of transport Q_{LSW} of a longshore sand wave can be estimated from the data set as:

$$(Q_{LSW})_{est,m} = \eta D V \quad (8)$$

in which η is the amplitude of the sand wave at a given calculation time step, and the quantity D is the sum of the depth of profile closure and the elevation of the active berm. The closure depth was taken as 6 m, and the elevation of the berm was 2 m.

The relation between the volume rate of longshore sand wave migration and the longshore discharge is taken as:

$$(Q_{LSW})_{Calc} = \alpha(R - R_{crit}) \quad (9)$$

and defines an empirical proportionality coefficient α. An estimate for the empirical coefficient α was obtained by substituting Eq. 8 into Eq. 9 and using representative values for observed sand wave speed and the hindcast wave conditions, giving $\alpha = 8.8 \times 10^{-4}$. This value represents an average over summer and winter wave conditions. The threshold value R_{crit} is unknown; for simplicity it was set equal to 2.4 $m^3 s^{-1}$ found for particulate transport (Kraus and Dean, 1987). R_{crit} for collective motion is probably larger, based on the results of Nasner (1974).

In the model, V is calculated at each time step from calculated breaking wave parameters and the amplitude of the sand wave at that time step, allowing the wave conditions to control the speed and direction of movement of the longshore sand wave on a time-dependent basis.

4.3. Wave model

The wave model of Kraus and Harikai (1983) was employed. At each calculation time step, the model refracts and shoals waves of specified height and direction over *locally* straight and parallel contours to breaking using the breaking criterion $H_b = 0.78\ d_b$, in which H_b is the wave height at breaking. An important feature of the wave model is what Kraus and Harikai called a "contour correction" to Snell's Law. By means of the contour correction, the orientation of the shoreline at each grid point alongshore is introduced into Snell's Law to the depth of closure; in the present situation, the contour correction in effect replicates the curvature of the subaerial portion of the sand wave in the offshore depth contours out to deep water where the waves are no longer effected by the bathymetry. As shown in Fig. 4, the bathymetry associated with the longshore sand waves is more complex than the simple assumption involving the shoreline shape, but the contour correction at least partially accounts for feedback between the local subaqueous morphology and the waves.

The contour correction causes waves to refract toward a longshore sand wave, much as waves tend to converge toward a headland. Convergence reduces the relative angle between the breaking waves and local shoreline, and as shown in Section 5, significantly reduces the degree of sand wave dispersion in the model runs.

4.4. Numerical solution scheme

Eq. 5 was solved by an explicit finite-difference method. Considerable effort was spent in determining the best representation of the advection term describing movement of the longshore sand wave. In independent tests, this term was represented by central differencing, linear upwind differencing, and the QUICK and QUICKEST (quadratic) upwind difference methods (Leonard, 1979). Without particulate longshore transport ($Q_P = 0$), allowing pure advection of a longshore sand wave, the central difference scheme showed persistent small oscillations at the base of the calculated wave, where it joined to straight shoreline, and standard linear upwind differencing introduced severe numerical diffusion. Of the QUICK and QUICKEST methods, the

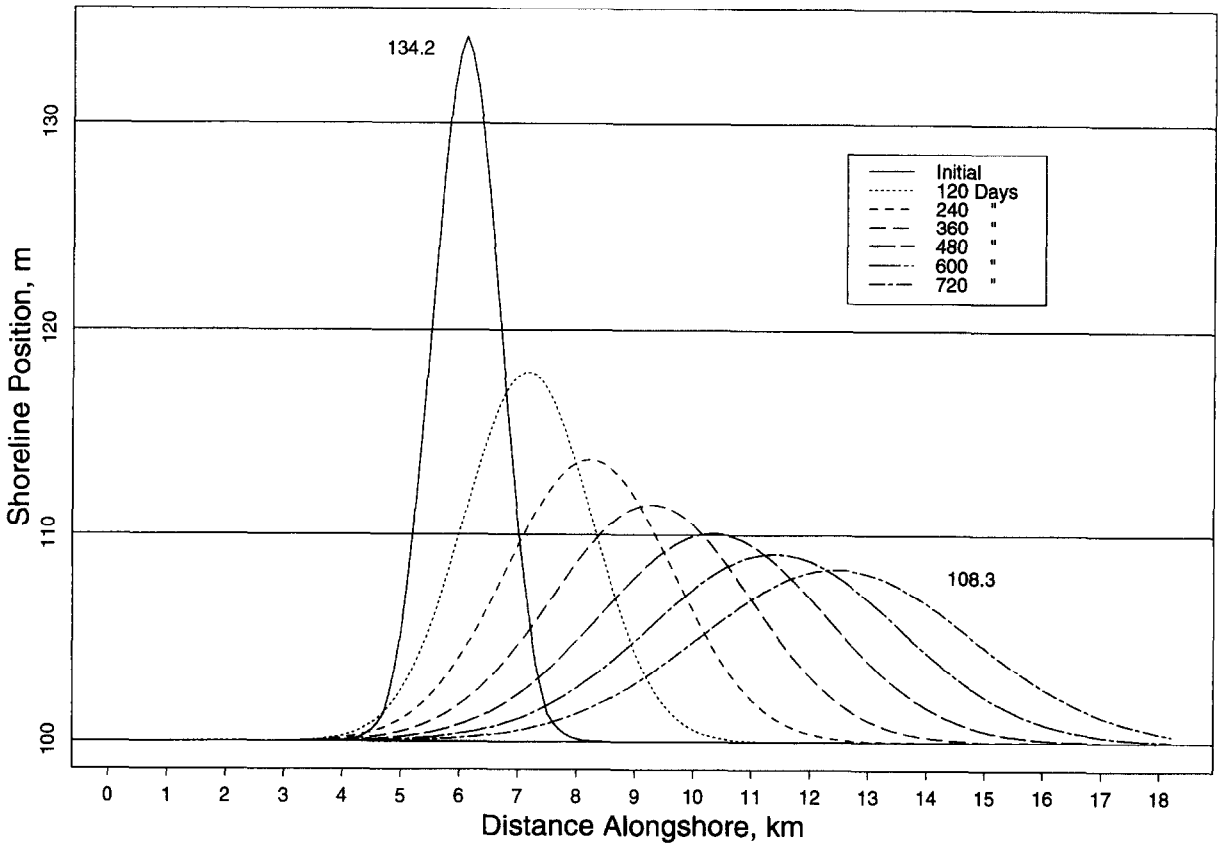

Fig. 8. Calculated longshore sand wave evolution without contour correction. (Full equation, no contour correction, $H=1$ m, $T=8$ s, direction 20°.)

QUICKEST method proved most stable and had little numerical diffusion. For pure advection of a longshore sand wave the size of LSW 3 under constant obliquely incident waves (1 m, 8 s, 20° angle at 20-m depth) for 4 months, the crest of the longshore sand wave decreased about 0.5 m. In the tests a time step of 3 h and uniform grid spacing of 50 m were used. Based on the test results, QUICKEST was employed.

5. Results

In reproducing observed longshore sand wave movement, a time step of 1 h and a grid spacing of 50 m were used. At each time step, a check was made to see if the Courant number exceeded 0.5 as described by Kraus and Harikai (1983). If the value 0.5 was exceeded, the time step was reduced by factors of 1/2 until the condition was satisfied. In this manner, arbitrary incident wave conditions as given by the WIS hindcast could be used with arbitrary shoreline configurations in automated manner without producing numerical instability.

In this study, the movement of a single longshore sand wave was investigated for clarity. The length of shoreline was taken as 18 km to eliminate boundary effects, and sand was allowed to move on and off of the grid by particulate transport. The dimensions of the initial form of the sand wave were that of LSW 3. The position of the shoreline was set at 100 m from an arbitrary baseline for ease of reading the plots. In the figures to follow, the reader should be aware of the large vertical exaggeration (approximately 350 to 1 in most figures).

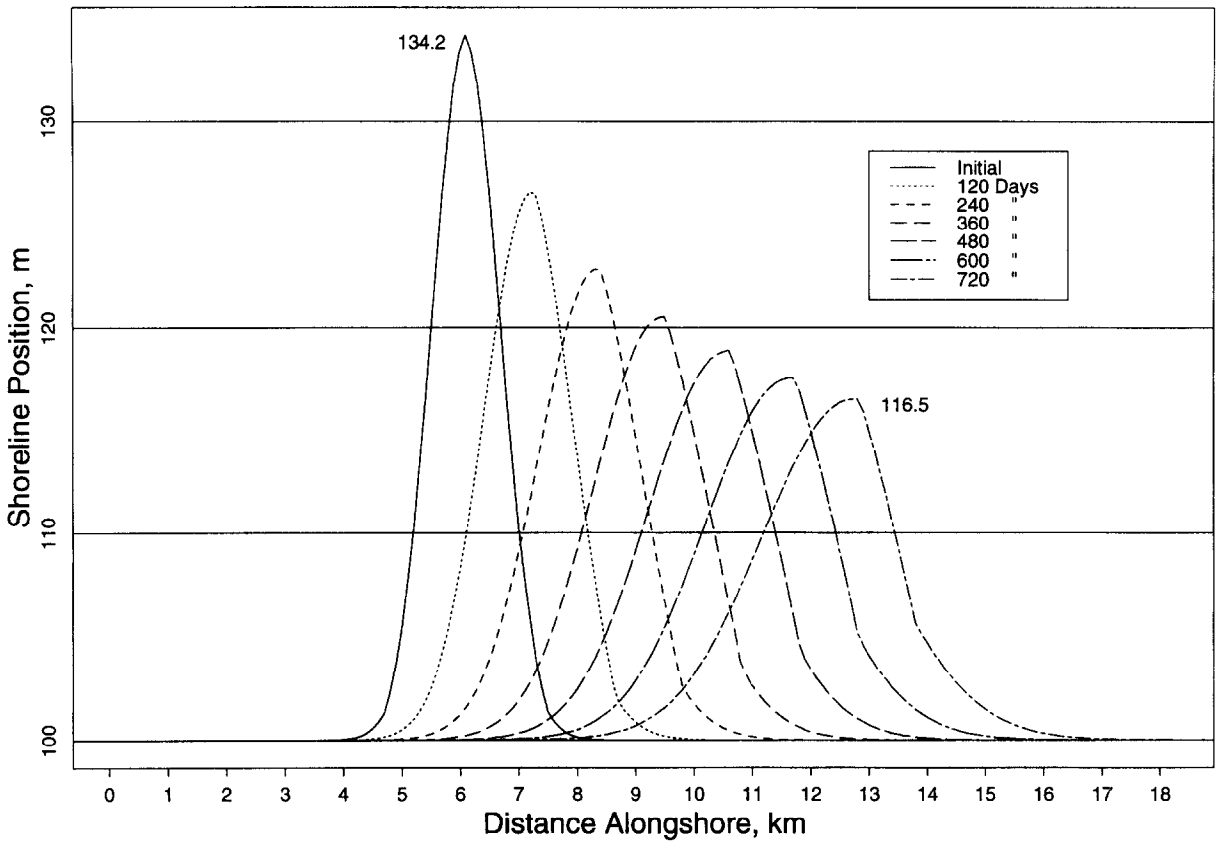

Fig. 9. Calculated longshore sand wave evolution with contour correction. (Full equation, $H=1$ m, $T=8$ s, direction 20°.)

5.1. Model tests

Many tests were performed to verify model predictions under symmetry of incident wave action, positive longshore sand wave shape, and reversed or negative wave shape (pure erosion wave). The model performed correctly in these tests.

Fig. 8 shows calculated longshore sand wave migration under constant incident wave action with the wave contour correction turned off. The incident waves in 10-m depth had significant height of 1 m, period of 8 s, and direction of 20°. With these strong and steady waves, after two years (an idealized year of 360 days was used) the crest of the longshore sand wave moved about 6 km. The entire sand wave body moved west, but there was significant decrease in amplitude, from 34.2 to 8.3 m, and extraordinary spreading was produced by the particulate transport term. The substantial spreading and decrease in amplitude are not in accord with the field observations.

The same case as above was run with the wave contour correction turned on, and the results are shown in Fig. 9. Compared to the case with the contour correction inoperative, the body of longshore sand wave remains much more intact and its amplitude decreases less, from 34.2 to 16.5 m. In addition, the longshore sand wave becomes asymmetrical, possessing a steeper flank downdrift in qualitative agreement with the field observations. Based on these and similar results, the contour correction is employed in subsequent calculations.

The next test shown is that for two half-year seasons, with summer waves for the first six months of height 0.5 m, period 8 sec, and direction −20° (waves directed to the east) and winter waves of

height 1 m, period 8 s, and direction 20° (waves directed to the west). The calculated results, output at 4-month intervals, are shown in Fig. 10. For the first four months of pure mild summer waves, the longshore sand wave moves less than 0.5 km to the east, and its decrease in amplitude is relatively small. The next 4-month interval includes two months of summer waves followed by two months of winter waves. The sand waves therefore experiences a net movement to the west, and the amplitude decreases somewhat more than in the first four months. The final 4-month increment contains purely winter waves, and the crest of the sand wave moves the most, approximately 1.3 km. This example shows that sand waves can move either east or west in the model, and that the translation speed and spreading of the sand wave are related to the incident wave characteristics.

5.2. *Simulation of observed sand-wave movement*

As previously mentioned, comparisons of calculated and observed evolution of only one longshore sand wave are presented for clarity. The period Sep. 1956–Jan. 1958 was used as input to the model, and incident waves were input for the 16-month observation period. As shown in Fig. 11, the observed sand wave (LSW 3) did not decrease in amplitude for the first four months, and it appeared to become narrower. For the same increment, the calculated sand wave moved in the correct direction (as it did for all time increments), but not quite as far. In addition, the calculated wave spread. The observed sand wave on Jan. 2, 1993 had a double peak at its crest, and the crest of the final calculated wave lies in the approximate center of these two peaks. Overall, reasonable

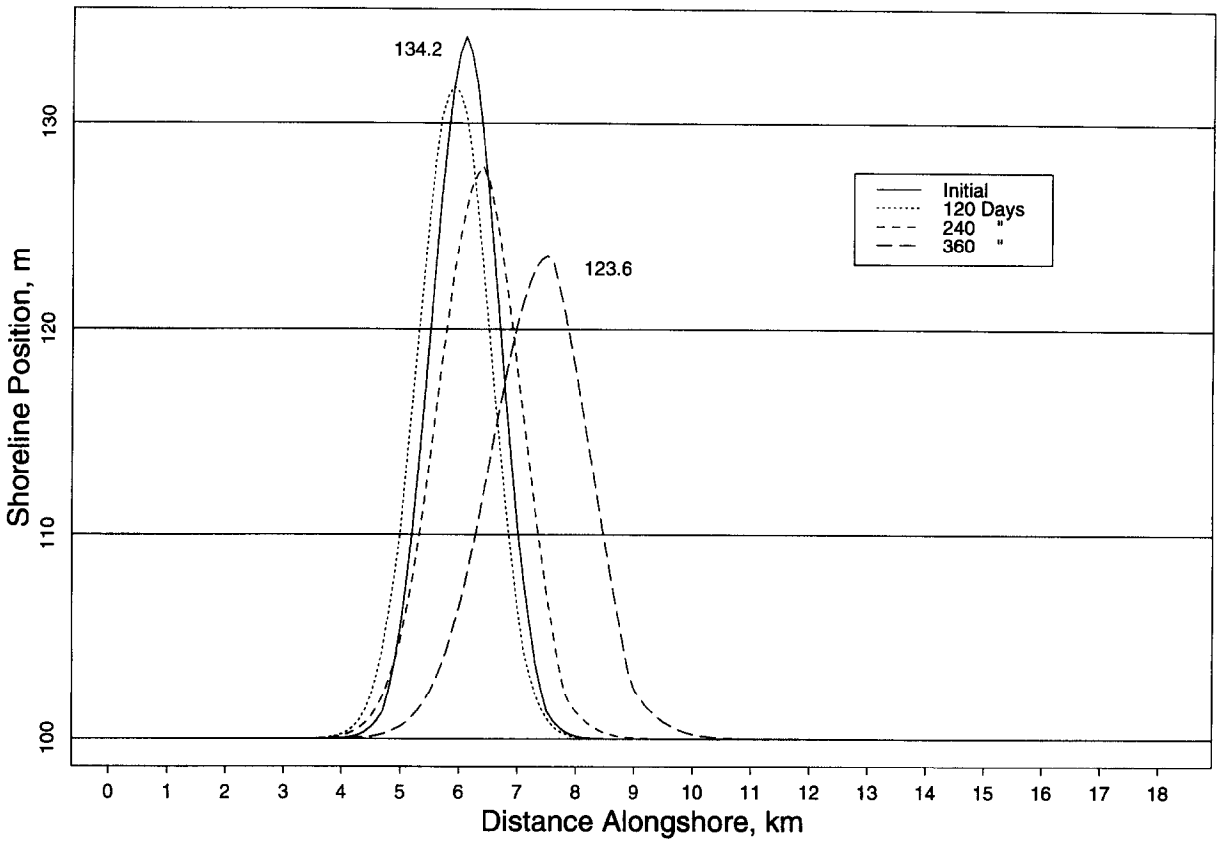

Fig. 10. Calculated longshore sand wave evolution for idealized seasonal waves. (Artificial seasons, Sum = 0.5 m, 8 s, −20°; Win = 1 m, 8 s, 20°.)

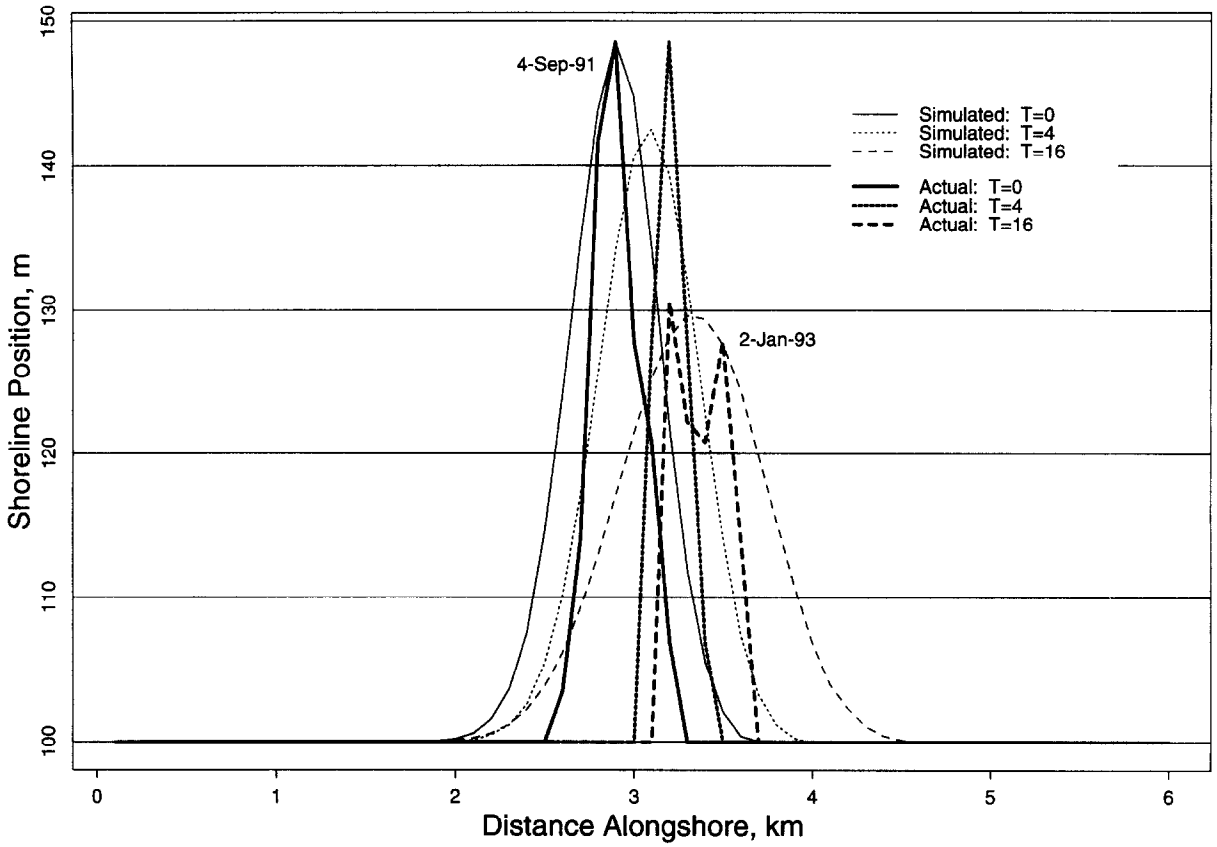

Fig. 11. Measured and calculated longshore sand wave movement. (Wave hindcast: Sep. year 1 to Jan. year 3).

quantitative agreement is seen, but with the calculated sand wave being too broad.

As shown in Fig. 11, the observed sand waves were much sharper in shape (seeming unnatural due to the vertical exaggeration of the plots) than the calculated waves. The initial form for the calculated sand wave was prepared from a narrower wave that was subjected to incident wave action to obtain the correct initial amplitude; the extra width and smoothness result from the spreading by particulate transport. A general characteristic of the model was to produce broader forms than observed.

6. Concluding discussion

In this study, multiple longshore sand waves were clearly tracked along Southampton Beach. The sand waves had an average length of 0.75 km and average amplitude of 40 m. Migration speed was greatest under winter waves and reached an average 1.09 km $year^{-1}$ in winter, whereas yearly average speed including summer calms was a much lower 0.35 km $year^{-1}$. During a 16-month observation period, the longshore sand waves did not disperse during steady migration westward in the direction of predominant wave incidence, and longer waves tended to move faster than those with smaller wavelengths.

A numerical simulation model was developed that reproduced many of the dynamic properties of longshore sand waves. The model contains transport contributions describing both individual (particulate) grain movement and collective movement of the sand body. The speed and direction of the sand waves were related to the longshore discharge of water, thereby giving the speed in a

predictive equation in terms of the incident wave conditions, sand wave amplitude and depth of closure. The single empirical coefficient in the transport rate formula was determined based on measured and calculated average conditions. The calculated sand waves moved more slowly in summer than winter, in agreement with observations.

An essential feature of the model is use of a contour correction, whereby the depth contours of the longshore sand wave are extended offshore, entering the wave refraction calculation. The contour correction causes incident water waves to converge on the sand wave, thereby reducing the sand-wave dispersion. The contour correction also reproduced the observed asymmetry in longshore sand wave form, which tends to show a steeper downdrift flank.

Refraction may also explain the longevity of observed sand waves. However, the calculated sand wave evolution showed more decrease in amplitude and more spreading than the observed sand waves. It is believed that one possible reason for less spreading in nature is that the subaqueous portion of the sand wave is more extensive than inferred from the subaerial portion. If this is true, than the basic shoreline modeling approach will have to be revised to allow non-uniformity in beach contours. Bathymetric surveys of longshore sand waves need to be made to provide information for improving our quantitative understanding and predictive capability.

The present study indicates that successful numerical simulation of longshore sand waves is likely possible, but detailed field surveys are required to provide needed information to progress in the mathematical description. Longshore sand waves are worthy of additional study because they are a simple form of collective sand body motion and because they are of engineering significance to such projects as shore protection and dredging of navigation channels.

Acknowledgements

We would like to thank Mr. Aram Terchunian, First Coastal Corporation, Westhampton Beach, for providing us with much information and insights on the longshore sand waves he has been observing at Southampton Beach. Also, we would like to thank Dr. Gary Zarillo, Florida Institute of Technology, for providing beach profile data and reports for the study site. This paper greatly benefitted from the comments of the reviewers and special issue editors, Drs. Jeffrey List and Joost Terwindt.

References

Bakker, W.T., 1968. A mathematical theory about sandwaves and its application on the Dutch Wadden Isle of Vlieland. Shore Beach, 36(2): 4–14.

Bruun, P., 1954. Migrating sand waves or sand humps, with special reference to investigations carried out on the Danish north coast sea. Proc. 5th Coastal Eng. Conf. ASCE, New York, pp. 269–295.

Evans, O.F., 1939. Mass transport of sediments on subaqueous terraces. J. Geol., 47: 324–334.

Grove, R.S., Sonu, C.J. and Dykstra, D.H., 1987. Fate of massive sediment injection on a smooth shoreline at San Onofre, California. Proc. Coastal Sediments '87. ASCE, New York, pp. 531–538.

Hanson, H. and Kraus, N.C., 1989. GENESIS: Generalized Model for Simulating Shoreline Change, Report 1: Technical Reference. Tech. Rep. CERC-89-19, U.S. Army Eng. Waterways Experiment Station, Coastal Eng. Res. Cent., Vicksburg, Miss.

Hicks, D.M. and Inman, D.L., 1987. Sand dispersion from an ephemeral river delta on the central California coast. Mar. Geol., 77: 305–318.

Hubertz, J.M., Brooks, R.M., Brandon, W.A. and Tracy, B.A., 1993. Hindcast wave information for the U.S. Atlantic coast. WIS Rep., 30, U.S. Army Eng. Waterways Experiment Station, Coastal Eng. Res. Cent., Vicksburg, Miss.

Inman, D.L., 1987. Accretion and erosion waves on beaches. Shore Beach, 55(3/4): 1073–1092.

Komar, P.D. and Inman, D.L., 1970. Longshore sand transport on beaches. J. Geophys. Res., 75(30): 5914–27.

Kraus, N.C. and Dean, J.L., 1987. Distributions of the longshore sediment transport rate measured by trap. Proc. Coastal Sediments '87. ASCE, pp. 881–896.

Kraus, N.C. and Harikai, S., 1983. Numerical model of the shoreline change at Oarai Beach. Coastal Eng., 7(1): 1–28.

Kraus, N.C. and Horikawa, K., 1990. Nearshore sediment transport. In: B. Le Mehaute and D. Hanes (Editors), The Sea; Ideas and Observations on Progress in the Study of the Seas. Wiley, New York, 9B, pp. 775–813.

Larson, M., Hanson, H. and Kraus, N.C., 1987. Analytical Solutions of the One-Line Model of Shoreline Change. Tech.

Rep. CERC-87-15, U.S. Army Eng. Waterways Experiment Station, Coastal Eng. Res. Cent., Vicksburg, Miss.

Larson, M. and Kraus, N.C., 1991. Mathematical modeling of the fate of beach fill. In: H.D. Niemayer, J. van Overeem and J. van de Graaff (Editors), Artificial Beach Nourishments. Spec. Issue Coastal Eng., 16: 83–114.

Leonard, B.P., 1979. A stable and accurate convective modeling procedure based on quadratic upstream interpolation. Computer Methods Applied Mech. Eng., 19: 59–98.

Leatherman, S.P. and Allen, J.R., 1985. Geomorphic analysis, Fire Island Inlet to Montauk Point, Long Island, New York. Final Rep. to U.S. Army Eng. District, New York.

Lockwood, Kessler and Bartlett, Inc., 1979. Cartographic analysis of Long Island, NY. Lockwood, Kessler and Bartlett, Syosset, New York.

Nasner, H., 1974. Prediction of the height of tidal dunces in estuaries. Proc. 14th Coastal Eng. Conf. ASCE, New York, pp. 1036–1050.

National Ocean Survey, 1992. Tide Tables—East Coast of North and South America, Including Greenland. NOAA, Rockville, MD.

Nersesian, G.K., Kraus, N.C. and Carson, F.C., 1992. Functioning of groins at Westhampton Beach, Long Island, New York. Proc. 23rd Coastal Eng. Conf. ASCE, New York, pp. 3357–3370.

Panuzio, F.L., 1968. The Atlantic coast of Long Island. Proc. 11th Coastal Eng Conf. ASCE, New York, pp. 1222–1241.

Pelnard-Considere, R., 1956. Essai de théorie de l'évolution des formes de rivage en plages de sable et de galets. 4th Journees de l'Hydraulique, Les Energies de la Mer, III(1), pp. 289–298.

Shore Protection Manual, 1984. U.S. Army Corps Eng., Coastal Eng. Res. Cent., U.S. Govt. Print. Off., Washington, DC. 2nd ed., 2 Vols.

Sonu, C.J., 1968. Collective movement of sediment in littoral environment. Proc. 11th Coastal Eng. Conf. ASCE, New York, pp. 373–398.

Terchunian, A., 1992. Beach and dune survey: post-dune restoration monitoring. Rep., First Coastal Corp., Westhampton Beach, NY. (Unpubl.)

Verhagen, H.J., 1989. Sand waves along the Dutch coast. Coastal Eng., 13: 129–147.

Zarillo, G.A. and Smith, G.L., 1986. Dynamics of Mecox Inlet and resulting effects on adjacent beaches. Rep., Mar. Sci. Res. Cent., SUNY Stony Brook, Stony Brook, NY. (Unpubl.)